Molecular Therapy
Nucleic Acids
Original Article

An mRNA-lipid nanoparticle vaccine targeting the *Plasmodium vivax* E140 antigen

Rodolfo Ferreira Marques,[1,2] Guilherme Antonio de Souza-Silva,[1] Vitor Antunes da Silva,[1] András Sárközy,[2] Máté Vadovics,[2] Hiromi Muramatsu,[2] Edit Ábrahám,[3,4] Carolina Bioni Garcia,[5] Silvia Beatriz Boscardin,[1] Rachel H.J. Jun,[6] Anna Caroline Campos Aguiar,[7] Zoltan Lipinszki,[3,4,8] Norbert Pardi,[2,9] and Daniel Youssef Bargieri[1,9]

[1]Department of Parasitology, Institute of Biomedical Sciences, University of São Paulo, São Paulo, São Paulo 05508-000, Brazil; [2]Department of Microbiology, Perelman School of Medicine, University of Pennsylvania, Philadelphia, PA 19104, USA; [3]Synthetic and Systems Biology Unit, Institute of Biochemistry, HUN-REN Biological Research Centre, 6726 Szeged, Hungary; [4]National Laboratory for Biotechnology, Institute of Genetics, HUN-REN Biological Research Centre, 6726 Szeged, Hungary; [5]Oswaldo Cruz Foundation, Leishmaniasis and Malaria Bioassay Platform, Porto Velho, Rondônia 76812-245, Brazil; [6]Acuitas Therapeutics, Vancouver, BC V6T 1Z3, Canada; [7]Department of Microbiology, Immunology, and Parasitology, Federal University of São Paulo, São Paulo, São Paulo 04023-062, Brazil; [8]ATGandCo Biotechnology Ltd, 6782 Mórahalom, Hungary

***Plasmodium vivax* (Pv) remains the primary cause of malaria outside Africa, yet no licensed vaccine is available against this pathogen. Here, we evaluate the immunogenicity and protective efficacy of novel vaccines targeting E140, a recently identified multi-stage antigen conserved across *Plasmodium* species. Lipid nanoparticle (LNP)-formulated nucleoside-modified mRNA vaccines against *P. berghei* E140 (PbE140) and *P. vivax* E140 (PvE140) induced robust antigen-specific IgG antibody responses, germinal center B cell, and long-lived plasma cell responses. Vaccination with PbE140 mRNA-LNP resulted in reduced parasitemia and improved survival in pathogen-challenged mice. Importantly, antibodies elicited by PvE140 mRNA-LNP in mice reduced invasion of primary human reticulocytes by *P. vivax* merozoites by 56%–78% in *ex vivo* functional assays. These findings suggest that E140 may be a promising antigen candidate for next-generation vaccines against *P. vivax*.**

INTRODUCTION

Malaria remains a global health challenge, with an estimated 263 million cases reported in 2023.[1] Within the *Plasmodium* genus, which comprises the protozoan species that cause malaria, *Plasmodium vivax* is a major contributor to malaria burden outside Africa, particularly in Southeast Asia and the Americas, given its wide geographic distribution and relapse biology.[1]

The implementation of artemisinin-based combination therapies for *Plasmodium falciparum* (*P. falciparum*) and chloroquine and primaquine for *P. vivax*, the use of rapid diagnostic tests, and the broad distribution of insecticide-treated bed nets have been crucial for reducing malaria incidence.[2] However, emerging resistance in mosquito vectors and parasites threaten the success of these strategies, contributing to a slowdown in the reduction of cases and potential future increases.[3,4] Vaccine development strategies against *Plasmodium* species target proteins that are critical in the parasite's life cycle at the pre-erythrocytic stage, blood stage, or sexual stage in the mosquito vector.[5] Currently, only two formulations are recommended for human use by the World Health Organization (WHO) against *P. falciparum*: the protein-based vaccines Mosquirix and R21/Matrix-M, both targeting the circumsporozoite protein (CSP).[6] Beyond their suboptimal efficacy (∼39% and ∼77%, respectively), both vaccines show waning protection over time, thus, requiring a multi-dose immunization schedule, have age- and schedule-specific implementation constraints, and their impact on transmission is limited.[6] These features underscore the need for further optimization and complementary vaccine strategies to achieve sustained population-level protection. Several *P. vivax* vaccine antigens are under investigation, such as PvCSP, duffy binding protein (PvDBP), and *P. vivax* 25-kDa surface protein (Pvs25)/*P. vivax* 230-kDa surface protein (Pvs230). Some have progressed to clinical trials,[5,7,8] but to our knowledge, no formulation has yet been found to provide robust and long-lasting protection against *P. vivax* malaria.

In the search for new potential vaccine antigens, a recent study showed that plasmid DNA prime followed by a boost with replication-incompetent human adenovirus 5 vector encoding the *Plasmodim yoelii* (*P. yoelii* E140) protein conferred 64% sterile protection in outbred CD1 mice and 100% sterile protection in BALB/c mice against both sporozoite and infected red blood cell challenges,[9]

Received 18 February 2026; accepted 1 September 2026;
https://doi.org/10.1016/j.omtn.2026.103083.

[9]These authors contributed equally

Correspondence: Norbert Pardi, Department of Microbiology, Perelman School of Medicine, University of Pennsylvania, Philadelphia, PA 19104, USA.
E-mail: pnorbert@pennmedicine.upenn.edu
Correspondence: Daniel Youssef Bargieri, Department of Parasitology, Institute of Biomedical Sciences, University of São Paulo, São Paulo, São Paulo 05508-000, Brazil.
E-mail: danielbargieri@usp.br

Published by Elsevier Inc. on behalf of The American Society of Gene and Cell Therapy.
This is an open access article under the CC BY-NC-ND license (http://creativecommons.org/licenses/by-nc-nd/4.0/).

suggesting broad vaccine coverage of the pre-erythrocytic and erythrocytic stages of the pathogen's life cycle. E140 has orthologs in several *Plasmodium* species, including *P. vivax* (Pv), and *P. berghei* (Pb), and in Pb it is expressed in distinct parasite forms such as mature sporozoites and late schizonts,[10] qualifying it as a promising target for multi-stage vaccine formulations.

Multiple immunization platforms have been explored for malaria vaccines, such as recombinant proteins, peptides, whole-parasites, and viral vectors.[5] More recently, nucleoside-modified mRNA in lipid nanoparticles (LNPs) has been used to develop malaria vaccines that allow rapid design and production, scalable manufacturing, and the induction of strong humoral and cellular immunity without handling live pathogens.[11]

Here, we used the nucleoside-modified mRNA-LNP vaccine platform to evaluate the immunogenicity and protective efficacy of the E140 antigen in mice. Animals were immunized with PbE140- or PvE140-encoding mRNA-LNP, and cellular and humoral immune responses and the protective efficacy of the vaccine formulations were evaluated.

RESULTS

PbE140 mRNA-LNP vaccination induces strong, persistent antibody responses

To evaluate the immunogenicity of mRNA-LNP vaccines encoding PbE140, BALB/c mice were intramuscularly (i.m.) immunized using two distinct vaccination regimens: two doses of 5 μg mRNA-LNP administered 30 days apart, or a single dose of 10 μg mRNA-LNP. Blood was collected one month after administration of each dose and 3 and 6 months after the last immunization. The control group received an irrelevant mRNA-LNP formulation encoding firefly luciferase (Luc). The PbE140 mRNA-LNPs induced robust antigen-specific IgG antibody responses in both groups, and antibody titers increased after administration of the boost. One month post last immunization, antibody titers were comparable in both PbE140 mRNA-LNP-injected experimental groups (Figure 1A).

IgG subclass analyses showed that IgG2a was the predominant subclass, and IgG2b titers were consistently lower (Figures 1B and 1C). Across dosing regimens, subclass profiles were broadly similar. IgG2a/IgG1 ratios were close to one in both groups (1 × 10 μg: 1.45; 2 × 5 μg: 1.11), demonstrating a mixed Th1/Th2 imprint rather than clearly a polarized response.

Antibody longevity analyses demonstrated sustained antigen-specific IgG (Figure 1D) and IgM (Figure 1E) titers through 6 months in both PbE140 immunization regimens. Together, these data indicate that our PbE140-encoding mRNA-LNP vaccine drives robust and durable humoral immunity in mice even after administration of a single vaccine dose.

PvE140 mRNA-LNP vaccination induces robust, persistent antibody responses

Immunizations of BALB/c mice with PvE140-encoding mRNA-LNP were performed as described for the PbE140 vaccination. The results were in line with those obtained with immunizations with PbE140 mRNA-LNP. Both immunization schemes elicited robust and comparable total antigen-specific IgG titers (Figure 2A) and subclass profiling showed a predominance of IgG2a (Figures 2B and 2C); IgG1 titers were comparable across the two-dose regimens (Figure 2C). IgG2a/IgG1 ratios were near one in both schedules (1 × 10 μg:1.68; 2 × 5 μg:1.07; Figures 2B and 2C), showing a broadly balanced Th1/Th2 profile. Total antigen-specific IgG (Figure 2D) and IgM (Figure 2E) titers followed through 6 months declined over time but, overall, remained high in the observation period.

PbE140 mRNA-LNP induces robust dose-dependent antigen-specific B cell responses

To characterize the B cell response induced by PbE140 mRNA-LNP vaccines, mice were immunized with these antigens following the two different dosing regimens as described previously. B cell responses were assessed from samples of spleen and bone marrow 30 days after the final immunization using surface antibody staining coupled with flow cytometric analysis (Figure S1A).

Antigen specificity was assessed by direct staining with recombinant PbE140/PvE140 protein (rPbE140/rPvE140) bearing a C-terminal hexahistidine tag (6×His), followed by anti-6×His-biotin antibody treatment, and detection with streptavidin to identify E140-binding cells within each B cell subset by flow cytometry. To provide comprehensive visualization of the complex multi-parameter flow cytometry data, TriMap dimensionality reduction analysis was applied to project the high-dimensional cellular data into a lower-dimensional space (Figure S1B). The TriMap visualizations effectively demonstrated the distribution patterns, clustering relationships, and population dynamics of different B cell subsets across all vaccination groups and tissue compartments, revealing distinct immunological landscapes for each experimental condition.

In the splenic compartment, PbE140 mRNA-LNP vaccines induced significantly elevated frequencies of total germinal center (GC) B cells compared to the Luc mRNA-LNP control group (Figure 3A). Consistent with this robust activation, PbE140-specific GC B cells accounted for a substantial fraction of the GC response, comprising approximately 25% of total GC B cells in mice immunized twice with 5 μg PbE140 mRNA-LNP and around 20% in those receiving a single immunization of 10 μg PbE140 mRNA-LNP (Figure 3B). Total plasma cell frequencies in the spleen were comparable between the PbE140-and Luc-immunized groups (Figure 3C). However, antigen-specific analysis revealed a striking difference, as PbE140-specific plasma cells constituted approximately ∼80% of total plasma cells in the PbE140 prime-boost group and around 60% in the single-dose PbE140 group (Figure 3D).

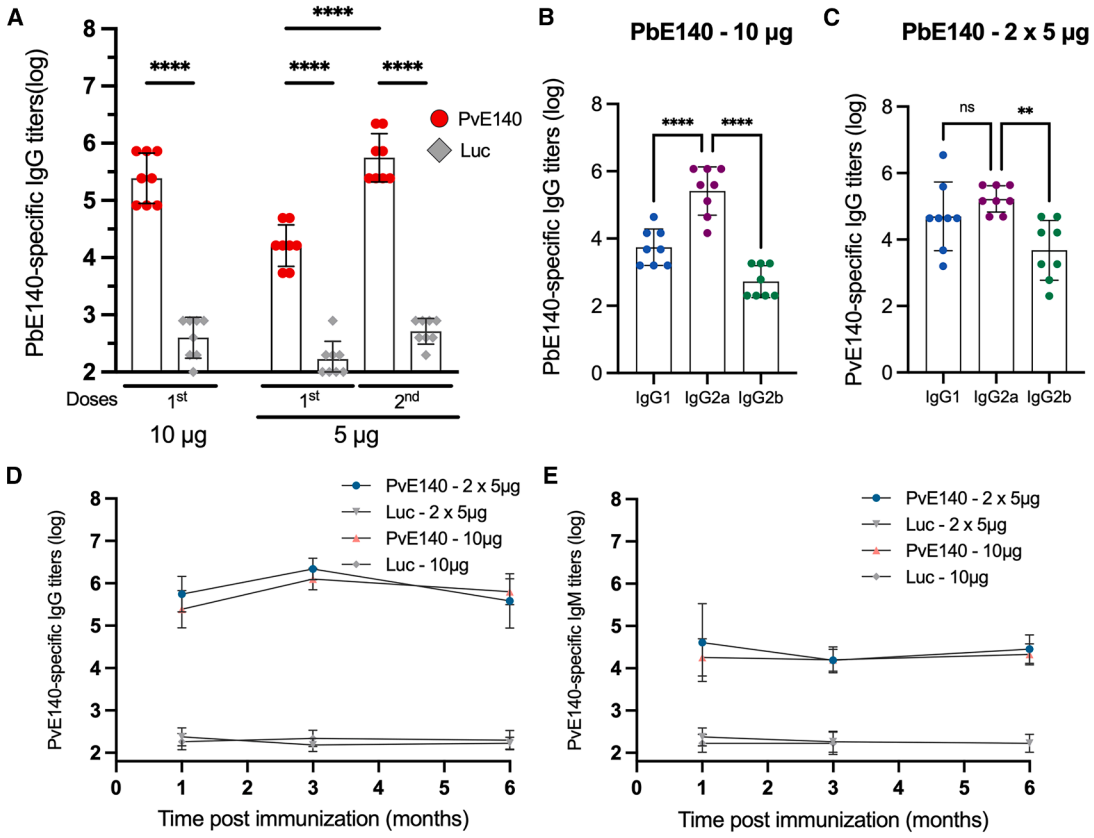


Figure 1. PbE140 mRNA-LNP vaccination induces strong, persistent antibody responses

Immunization scheme: BALB/c mice received a single intramuscular dose of 10 µg PbE140 or Luc mRNA-LNP or two doses of 5 µg PbE140 or Luc mRNA-LNP given 30 days apart. Retro-orbital blood collections were performed 1, 3, and 6 months after last immunization. (A) Total anti-PbE140 IgG endpoint titers were determined 1 month after last immunization by ELISA. (B) IgG subclass profiles (IgG1, IgG2a, IgG2b) in groups receiving a single 10 µg dose 1 month after last immunization. (C) IgG subclass profiles (IgG1, IgG2a, IgG2b) in groups receiving two immunizations with 5 µg at the indicated time points. (D) IgG longevity against PbE140 for 6 months after administration of the last vaccine dose. (E) IgM longevity against PbE140 for 6 months after administration of the last vaccine dose. For (A–C), each symbol represents one animal, data shown as mean ± SD ($n = 8$ mice per group). Results are expressed as the geometric mean titers in log10 ± SD and the data were statistically analyzed using one-way ANOVA followed by Tukey's test. Significant differences among groups are indicated on the graph as $^{**}p < 0.01$, $^{****}p < 0.0001$. Non-significant (ns) differences are indicated as $p > 0.05$.

Similarly, total plasmablast frequencies did not differ significantly between the PbE140 and Luc mRNA-LNP-vaccinated groups (Figure 3E). Despite this finding, PbE140-specific plasmablasts represented a large proportion of the antibody-secreting cell compartment, accounting for approximately 60% of total plasmablasts in mice immunized twice with 5 µg PbE140 mRNA-LNP, compared to around 30% in those receiving a single dose of 10 µg PbE140 (Figure 3F). In the bone marrow compartment, a critical anatomical niche for the establishment and maintenance of long-lived plasma cells, PbE140 mRNA-LNP vaccination induced total plasma cell frequencies of up to ∼2% in both the prime-only and prime-boost groups (Figure 3G). Notably, PbE140-specific plasma cells dominated this compartment, comprising more than ∼95% of total plasma cells in mice that received 2 doses of PbE140 mRNA-LNP (Figure 3H). Total plasmablast frequencies in the bone marrow remained relatively low and consistent across all vaccination groups, ranging between ∼0.1% and ∼0.2% (Figure 3I). Nevertheless, among mice immunized twice with PbE140 mRNA-LNP, the vast majority of plasmablasts detected were PbE140-specific, with PbE140-binding cells accounting for more than 95% of the total plasmablast population (Figure 3J).

Overall, these data demonstrate that PbE140 mRNA-LNP vaccination induces highly focused antigen-specific humoral responses, with two immunizations consistently exhibiting superior immunogenicity compared to administration of a single vaccine dose.

PvE140 mRNA-LNP induces modest dose-dependent antigen-specific B cell responses

The immunization with mRNA vaccines encoding *P. vivax* E140 followed the same experimental parameters used for PbE140 (Figures S2A and S2B), allowing direct assessment of the immunogenic potential of its *P. vivax* ortholog. The PvE140 dosing regimens induced robust total GC B cell responses in the spleen following immunization with either two doses of 5 µg or a single immunization of

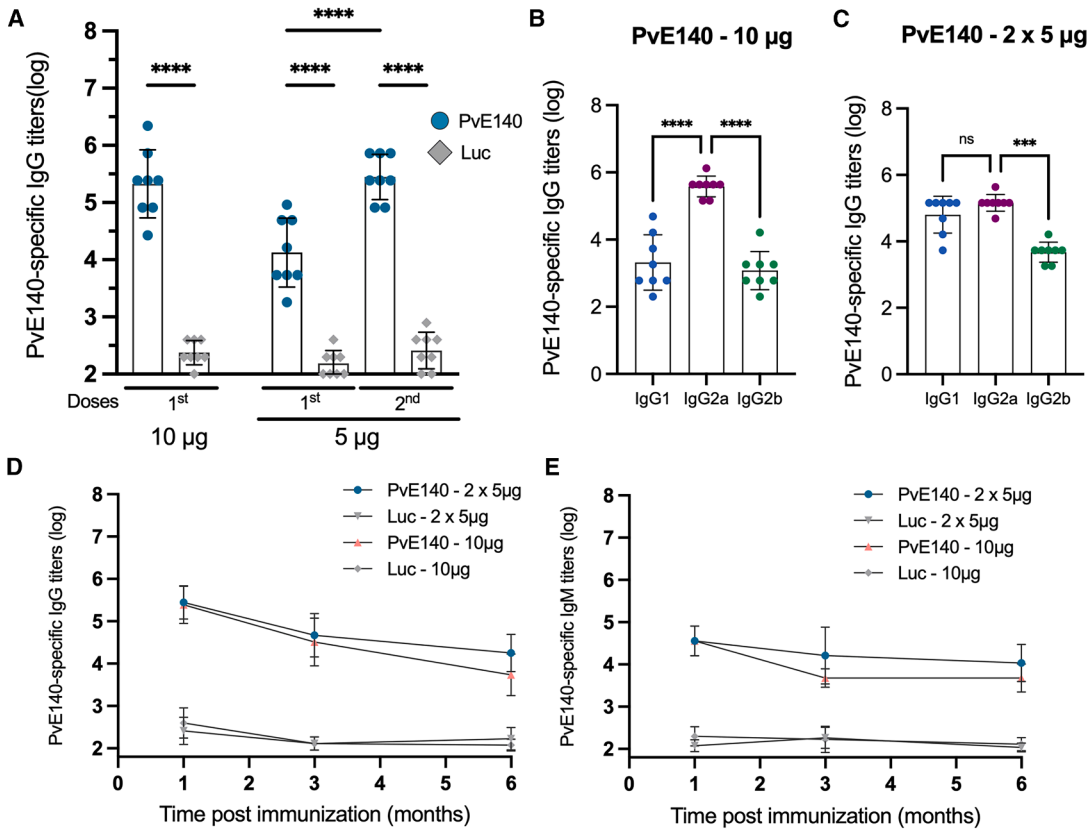


Figure 2. PvE140 mRNA-LNP vaccination induces strong, persistent antibody responses

Animals were immunized with PvE140 and Luc mRNA-LNPs as described in Figure 1 for PbE140 and Luc mRNA-LNP. Retro-orbital blood collections were performed 1, 3, and 6 months after last immunization. (A) Total anti-PvE140 IgG endpoint titers were measured over time by ELISA. (B) IgG subclass profiles (IgG1, IgG2a, IgG2b) in groups receiving a single immunization at the indicated time points. (C) IgG subclass profiles (IgG1, IgG2a, IgG2b) in groups receiving two immunizations at the indicated time points. (D) IgG longevity against PvE140 up to 6 months after administration of the last vaccine dose. (E) IgM longevity against PvE140 up to 6 months after administration of the last vaccine dose. For (A–C), each symbol represents one animal, data shown as mean ± SD ($n = 8$ mice per group). Results are expressed as the geometric mean titers in log10 ± SD and the data were statistically analyzed using one-way ANOVA followed by Tukey's test. Significant differences among groups are indicated on the graph as, ***$p < 0.001$, ****$p < 0.0001$. Non-significant (ns) differences are indicated ($p > 0.05$).

10 µg (Figure 4A). Despite this strong overall activation, the frequency of PvE140-specific GC B cells was limited, comprising approximately ∼2%–3% of total GC B cells in both vaccination regimens (Figure 4B).

Consistent with these findings, PvE140 vaccination also elicited substantial total plasma cell responses in the spleen (Figure 4C). However, antigen-specific plasma cells represented only a small proportion of the total plasma cell pool, with PvE140-specific plasma cells accounting for approximately ∼1% of total plasma cells in mice immunized twice with 5 µg or receiving a single dose of 10 µg (Figure 4D). A similar pattern was observed for plasmablast responses. PvE140-immunized mice showed robust total plasmablast frequencies (Figure 4E), whereas PvE140-specific plasmablasts constituted only ∼1% of total plasmablasts in both vaccination groups (Figure 4F).

In the bone marrow compartment, PvE140 vaccines induced high frequencies of total plasma cells in both the prime-only and prime-boost groups (Figure 4G). Nevertheless, PvE140-specific plasma cells remained scarce, representing approximately ∼0.3% of total plasma cells in both groups (Figure 4H). Finally, PvE140 vaccination promoted substantial total plasmablast responses in the bone marrow (Figure 4I), although antigen-specific plasmablasts accounted for only ∼1.25% of total plasmablasts across both vaccination strategies (Figure 4J).

Overall, these data indicate that PvE140 vaccination induces strong B cell activation in both the spleen and bone marrow but results in limited antigen-specific differentiation, suggesting that although PvE140 mRNA-LNP is immunogenic, it elicits a less focused humoral response compared to PbE140 mRNA-LNP in mice.

PbE140 mRNA-LNP vaccination reduces parasitemia and improves survival rates in parasite-challenged mice

To test whether the PbE140 mRNA-LNP vaccine protects mice against *Plasmodium* infection, animals were vaccinated with the

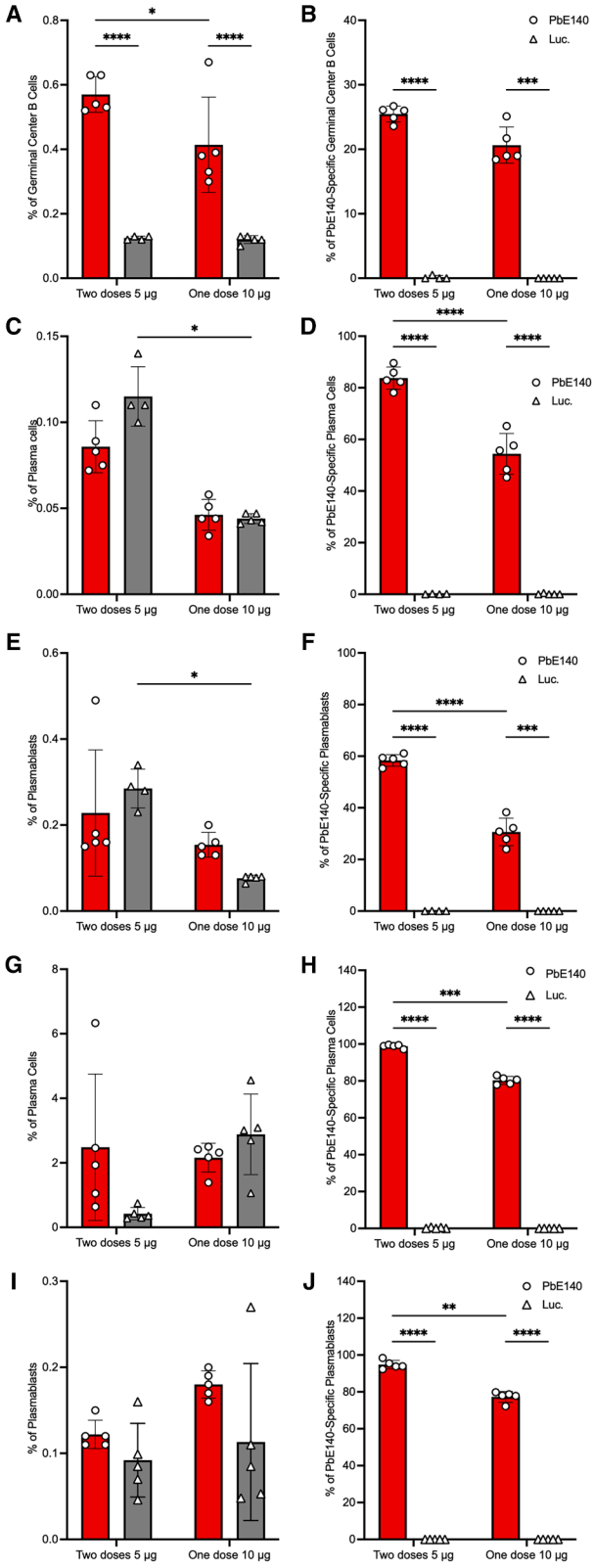


Figure 3. PbE140 mRNA-LNP induces robust dose-dependent antigen-specific B cell responses

Thirty days after the last immunization, spleens and bone marrow were harvested, and 2 × 10^6 cells from each compartment were processed for surface staining and flow cytometric analysis. Sequential gating strategy was employed to identify B cell subpopulations. Following exclusion of dead cells using live/dead discrimination and lymphocyte identification based on scatter characteristics, $CD3^+$ T cells were excluded to focus on the $B220^+$ B cell compartment. Germinal center (GC) B cells were defined as $B220^+GL7^+CD95^+$, plasmablasts as $B220^+CD138^+$, and plasma cells as $B220^-CD138^+$. Antigen specificity was determined through direct staining with 5 µg/mL recombinant PbE140 protein. (A–E) Frequency of total B cell subpopulations in the spleen: (A) GC B cells ($B220^+GL7^+CD95^+$), (C) plasma cells ($B220^-CD138^+$) and (E) plasmablasts ($B220^+CD138^+$). (B–F) Frequency of PbE140-specific B cell subpopulations in the spleen: (B) PbE140-specific GC B cells, (D) PbE140-specific plasma cells, and (F) PbE140-specific plasmablasts. (G–I) Frequency of total B cell subpopulations in the bone marrow: (G) plasma cells ($B220^-CD138^+$) and (I) plasmablasts ($B220^+CD138^+$). (H–J) Frequency of PbE140-specific B cell subpopulations in the bone marrow: (H) PbE140-specific plasma cells and (J) PbE140-specific plasmablasts. (A, C, E, G, and I) Show the total percentage of B cell populations indicated on the *y* axis. (B, D, F, H, and J) Show the percentage of PbE140-specific B cells within the corresponding total population, according to the hierarchy of gates used in flow cytometry analysis (Figures S1A). Each symbol represents one animal. Data are presented as individual values with mean ± SD (n = 5 animals per group). Statistical analysis was performed using one-way ANOVA followed by Tukey's post hoc multiple comparisons test. Significant differences are indicated in the figure as: *$p < 0.05$, **$p < 0.01$, ***$p < 0.001$, and ****$p < 0.0001$.

two different dosing regimens as described previously and were challenged 30 days after the last immunization with Pb NK65 using 5 × 10^3 infected red blood cells. Blood samples were taken every other day from day 4 to day 40 after the challenge to monitor parasitemia by microscopy. Both vaccination regimens, single dose of 10 µg (Figures 5A and 5B) or two doses of 5 µg (Figures 5C and 5D), reduced parasitemia (Figures 5A and 5C) and improved survival of the animals (Figures 5B and 5D) after challenge. Moreover, naive mice that received sera from PbE140 mRNA-LNP-immunized donors prior to challenge (Figure 5E) had lower blood parasite burden compared to naive mice that received sera from Luc mRNA-LNP-immunized controls. The $\log_{10}$ area under the curve (AUC) of parasitemia was significantly lower in recipients of PbE140 immune sera than in Luc controls ($p < 0.0001$) (Figures 5F and 5G). These results suggest that the protection induced by the PbE140 mRNA-LNP vaccines is, at least in part, antibody-mediated. This is in line with our findings showing localization of the E140 protein on the surface of Pb merozoites (Figure S3) that can potentially be targeted by neutralizing or opsonizing antibodies.

Antibodies induced by PvE140 mRNA-LNP can inhibit *P. vivax* merozoite invasion of human reticulocytes

To assess the protective potential of the PvE140 mRNA-LNP vaccine, re-invasion assays of human primary reticulocytes with *P. vivax* isolates were conducted in the presence of sera from mice immunized twice with 5 µg PbE140 or Luc mRNA-LNP. In three independent experiments, the PvE140 immune serum reduced *P. vivax* reticulocyte invasion by 78%, 56%, and 60% when compared to invasion rates in the presence of the Luc control serum (Figure 6A). In assays with Luc control serum, young trophozoites were found developing

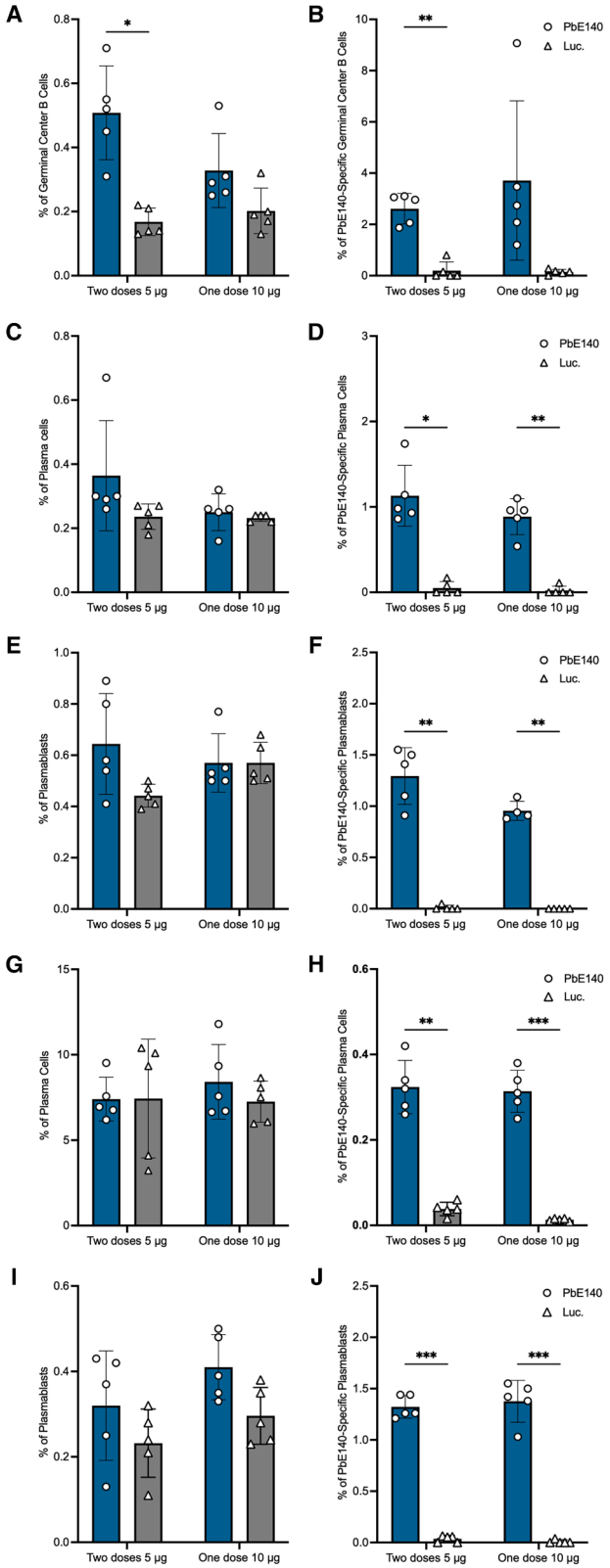


Figure 4. PvE140 mRNA-LNP elicits modest antigen-specific B cell responses

Thirty days after the last immunizations, spleens, and bone marrow were harvested, and 2 × 10^6 cells from each compartment were processed for flow cytometric analysis. The analysis reveals distinct clustering patterns and population distributions specific to PvE140 vaccine responses. (A–E) Frequency of total B cell subpopulations in the spleen: (A) GC B cells ($B220^+GL7^+CD95^+$), (C) plasma cells ($B220^-CD138^+$), and (E) plasmablasts ($B220^+CD138^+$). (B–F) Frequency of PvE140-specific B cell subpopulations in the spleen: (B) PvE140-specific GC B cells, (D) PvE140-specific plasma cells and (F) PvE140-specific plasmablasts. (G–I) Frequency of total B cell subpopulations in the bone marrow: (G) plasma cells ($B220^-CD138^+$) and (I) plasmablasts ($B220^+CD138^+$). (H–J) Frequency of PvE140-specific B cell subpopulations in the bone marrow: (H) PvE140-specific plasma cells and (J) PvE140-specific plasmablasts. (A, C, E, G, and I) Show the total percentage of B cell populations indicated on the *y* axis. (B, D, F, H, and J) Show the percentage of PvE140-specific B cells within the corresponding total population, according to the hierarchy of gates used in flow cytometry analysis (Figures S2A). Each symbol represents one animal. Data are presented as individual values with mean ± SD (n = 5 animals per group). Statistical analysis was performed using one-way ANOVA followed by Tukey's post hoc multiple comparisons test. Significant differences are indicated in the figure as: *$p < 0.05$, **$p < 0.01$, ***$p < 0.001$, and ****$p < 0.0001$.

inside reticulocytes (Figure 6B), whereas in PvE140 immune serum-treated assays, a phenotype of a merozoite bound to a reticulocyte was frequently recorded (Figure 6C) and represented 32% of all observed parasite-RBC interactions. This phenotype was not seen in the Luc control-treated samples. Collectively, these data show that antibodies targeting PvE140 inhibit *P. vivax* merozoite invasion of human reticulocytes.

DISCUSSION

Malaria elimination remains a challenge and no vaccine is available against *P. vivax*, which is widely spread in all tropical regions outside Africa. Its genetic-antigenic diversity complicate vaccine development and highlights the need for new antigens and vaccine platforms that elicit durable immunity.[5,12,13] Here, we show that the E140 protein is a promising antigen for the development of *P. vivax* malaria vaccines using the nucleoside-modified mRNA-LNP platform, which has been recently proposed as a promising modality for next-generation *P. vivax* vaccines using Pvs25 and CSP as antigens.[14,15]

Previous studies suggest that the *Plasmodium* E140 protein may represent a biologically important vaccine target. Proteomic and reverse-genetics approaches identified E140 orthologs across *Plasmodium* species and indicated expression in multiple developmental stages, including sporozoites and blood stages.[16] In addition, targeted gene disruption attempts of the Pb ortholog repeatedly failed in independent experiments, suggesting that E140 may be essential for parasite survival or development during the blood stage.[16] Although the precise role of PbE140 during parasite development remains unresolved, these observations further suggest that E140 is a biologically relevant vaccine target.

In our studies, both the prime-only immunization with 10 µg E140-encoding mRNA-LNP and the prime-boost vaccination with 5 µg

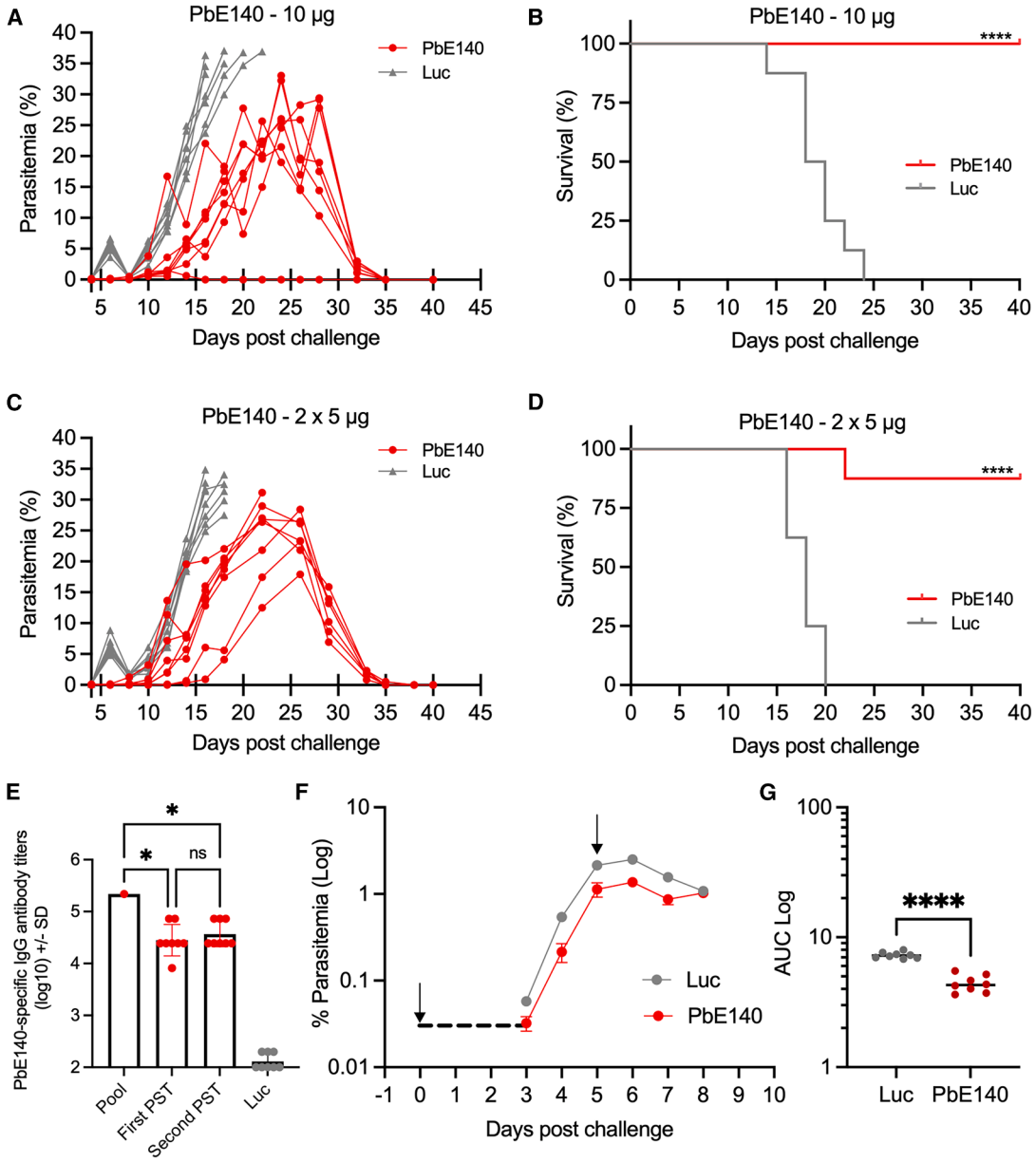


Figure 5. PbE140 mRNA-LNP vaccination reduces parasitemia and improves survival rates in parasite-challenged mice

Immunization and challenge timeline: BALB/c mice were immunized as described for Figure 1 (n = 8/group). Challenge was performed intravenously with 5×10^3 *P. berghei* NK65-infected red blood cells 1 month after the last immunization, and parasitemia was monitored by Giemsa-stained thin blood smears every other day starting 4 days post-challenge. Survival curves were compared to the Luc control using the Mantel-Cox (log rank) test. Significant differences are indicated in the figure as ***$p < 0.001$ and ****$p < 0.0001$. (A) Parasitemia kinetics for the prime-only cohort. Each line represents one mouse; data are shown as percent parasitemia. (B) Survival curves for the prime-only cohort. (C) Parasitemia kinetics for the prime-boost cohort. Each line represents one mouse; data are shown as percent parasitemia. (D) Survival curves for the prime-boost cohort. (E) Anti-PbE140 IgG titers measured in pooled donor serum from BALB/c mice immunized twice with 5 µg PbE140 mRNA-LNP vaccine and in recipient BALB/c mice approximately 8 h after the first and second passive serum transfer (PST). The first PST was performed 2 h before parasite challenge, and the second PST was performed 5 days after challenge. Recipients received 200 µL of serum at each transfer. Each symbol represents one mouse. Antibody titers are expressed as $\log_{10}$ endpoint titers determined by ELISA. Significant differences are indicated as *$p < 0.05$; ns, not significant. (F) Passive serum transfer. Naive recipient BALB/c mice (n = 8) received 200 µL of pooled sera via the retro-orbital route on day 0 and day 5 from donors previously immunized with two doses of 5 µg PbE140 or Luc mRNA-LNP and collected 30 days after the last immunization. Recipients were challenged intravenously with 5×10^3 *P. berghei* NK65-infected red blood cells 8 h after the first serum transfer, and parasitemia was quantified from day 3 to day 8 by Giemsa-stained blood smears. Arrows indicate the timing of serum administration. (G) Parasite burden after passive transfer was expressed as the area under the parasitemia curve (AUC) calculated from days 3 to day 8 post-challenge. Bars represent mean ± SD. Group comparisons were performed using a two-tailed unpaired t test. ****$p < 0.0001$.

mRNA-LNP elicited high anti-E140 IgG antibody titers that were durable over 6 months post immunization in mice, demonstrating that the nucleoside-modified mRNA-LNP vaccine platform can induce robust and long-lasting humoral immunity.

IgG subclasses mirror helper T cell polarization. In BALB/c mice (Th2-skewed), IgG1 typically exceeds IgG2a[17–20]; in our studies, IgG2a/IgG1 ratios clustered near 1.0 with the prime-boost regimen, indicating a mixed Th1/Th2 response, and were higher in the single dose regimen, suggesting a slightly more Th1-biased response. Although Th1-associated IgG2a is often linked to protection in murine malaria,[21,22] and human IgG1/IgG3 equivalent murine IgG2a in functional correlates,[23–28] subclass proportions alone are unlikely to determine vaccine efficacy, as additional antibody features including epitope specificity, affinity/avidity, and Fc-mediated functions also contribute to protection. While immunization once with 10 μg PbE140 mRNA-LNP showed the highest IgG2a titers and was associated with complete survival following challenge, this observation should be interpreted cautiously and does not alone establish a causal relationship between IgG2a levels and protection. Most vaccine studies against malaria have predominantly focused on the induction of IgG responses, as class switching from IgM to IgG is often associated with affinity maturation and improved effector functions.[29] However, IgM can contribute to antimalarial protection: passive transfer of anti-CSP IgM conferred 74% protection in *P. yoelii*-infected BALB/c mice,[30] and in human *P. falciparum* infection, IgM is rapidly induced and inhibits erythrocyte invasion via complement fixation on merozoites.[31] Consistent with these observations, SumayaVac-1 (using full-length MSP1 antigen) elicited functional IgG and IgM that activated classical complement, promoted opsonophagocytosis, and engaged IFN-γ/NK cell effector pathways.[32] In our study, both PbE140 and PvE140 mRNA-LNP vaccines induced high anti-E140 IgM titers with notable durability for at least 6 months, raising that mRNA vaccine-induced IgM may contribute to the observed protection along with IgG-mediated mechanisms.

Nucleoside-modified mRNA-LNP vaccines can induce persistent GC responses that drive affinity maturation and the establishment of long-lived plasma cells in survival niches.[33,34] The bone marrow represents a critical site for plasma cells, where they can persist for extended periods and maintain sustained antibody production.[35] The high frequency of E140-specific cells in this compartment suggests that the PbE140 mRNA-LNP vaccine establishes the cellular foundation of durable humoral immunity. This finding is particularly significant given that correlates of protection for many vaccines depend on functional antibodies that block infection or pathogen dissemination,[36] and the persistence of antigen-specific plasma cells in the bone marrow is a key determinant of long-term protective immunity.[37]

The different immunogenicity of the PbE140 and PvE140 mRNA-LNP vaccines (despite their structural similarity and identical delivery platform) underscores the importance of antigen characteristics

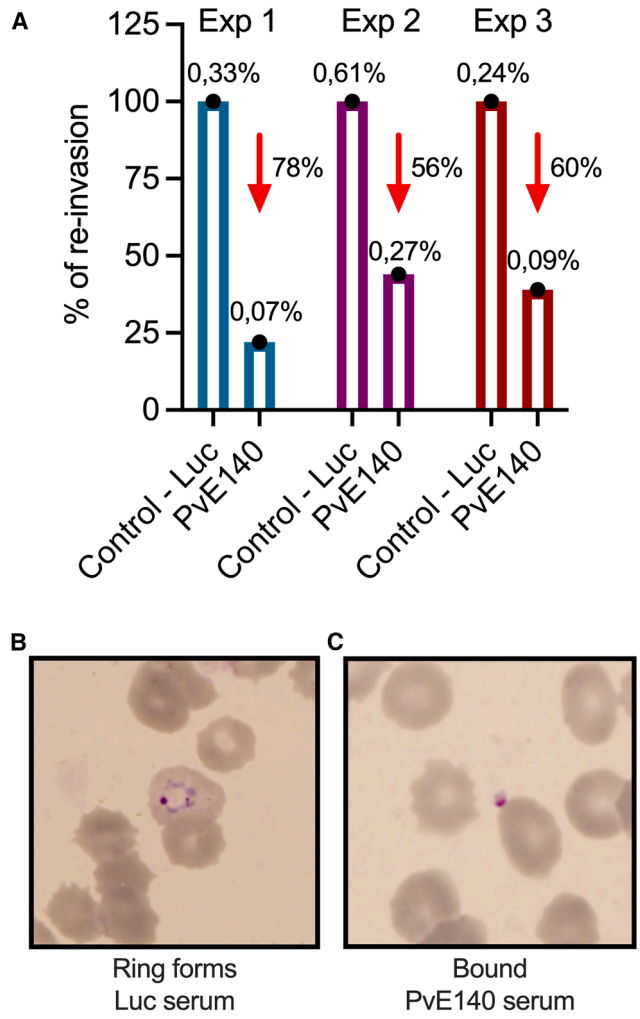


Figure 6. Antibodies induced by PvE140 mRNA-LNP can inhibit *P. vivax* merozoite invasion of human reticulocytes

(A) Percent re-invasion in three independent experiments using serum samples collected 30 days after the last immunization from BALB/c mice that received two times 5 μg doses of either PvE140 mRNA-LNP or Luc mRNA-LNP. For each experiment, the Luc group was set to 100% re-invasion, and inhibition in the PvE140 group was calculated relative to its paired control. Numbers above bars indicate the absolute ring-stage parasitemia measured on blood smears (e.g., Exp.1: 0.33% vs. 0.07%; Exp.2: 0.61% vs. 0.27%; Exp.3: 0.24% vs. 0.09%). Red arrows denote the corresponding percent inhibition (Exp.1: 78%, Exp.2: 56%, Exp.3: 60%). (B) Representative Giemsa-stained field showing ring-stage parasites within reticulocytes following successful re-invasion in assays incubated with sera from Luc mRNA-LNP-immunized mice. (C) Representative Giemsa-stained field showing a merozoite bound to a reticulocyte with no evidence of invasion after 30 h of assays incubated with sera from PvE140 mRNA-LNP-immunized mice.

in determining vaccine efficacy. While both vaccines induced antigen-specific B cell responses, the PvE140 vaccine generated substantially lower frequencies of antigen-specific cells across all measured parameters. This disparity may reflect intrinsic differences in protein structure, epitope accessibility, or immunodominance patterns

between these two E140 orthologs. Such antigen-dependent variations in immunogenicity have been observed in other vaccine platforms and highlight the need for careful antigen optimization in vaccine design.[38] The robust GC responses induced by both vaccines, as evidenced by the substantial frequencies of $GL7^+CD95^+$ B cells, indicate that the nucleoside-modified mRNA-LNP platform effectively promotes the formation of these critical immune microenvironments where affinity maturation occurs.[33] However, the marked differences in antigen specificity within these GCs suggest that the quality of the immune response, rather than just its magnitude, is fundamentally influenced by the antigen being presented.

Although PvE140 and PbE140 mRNA-LNP vaccinations induced comparable serum antibody titers, PvE140 generated lower frequencies of detectable antigen-specific plasma cells. This apparent discrepancy may reflect differences in the kinetics or qualitative features of the B cell response rather than a reduced humoral response. While plasma cell frequencies represent a snapshot of a specific cellular compartment at the time of analysis, serum antibody titers reflect cumulative antibody production over time. In addition, differences in antigen properties, including conformation or epitope accessibility, may influence the differentiation or detection of antigen-specific B cell populations without necessarily affecting overall antibody titers.

In some of the immunological readouts assessed in this study, prime-boost immunizations outperformed single-dose vaccinations, suggesting their preferred use for mRNA-based malaria vaccines. Repeated antigen exposure increases both the magnitude and quality of immune responses by sustaining GCs and driving somatic hypermutation that enhances antibody affinity.[34,39]

Importantly in functional *ex vivo* re-invasion assays that can inform about the protective efficacy of vaccine-induced antibodies in humans, immune sera raised by PvE140 mRNA-LNP curtailed merozoite invasion into primary human reticulocytes in three independent experiments with up to 78% inhibition, indicating that vaccination elicits antibodies with direct neutralizing activity against the erythrocytic cycle of *P. vivax*. The potent invasion inhibition achieved by PvE140 antisera is comparable to those observed with antibodies targeting leading *P. vivax* blood stage vaccine candidates, like PvDBP and the reticulocyte binding protein 2b (RBP2b). Specifically, rabbit polyclonal antibodies to the region II of DBP (PvDBPII) reduced the number of new ring-stage infections from Thai clinical isolates by up to 64% in short-term *ex vivo* invasion assays, and pooled human PvDBPII antisera from *P. vivax*-exposed individuals achieved up to 54% inhibition of reticulocyte invasion.[40] Monoclonal antibodies (mAbs) against PvDBPII that block the interaction of DBPII with its receptor, the duffy antigen receptor for chemokines (DARCs), reduced reticulocyte invasion by up to 70% in *ex vivo* assays using Brazilian and Cambodian isolates,[41] and mAbs targeting the transferrin receptor-1-binding domain in RBP2b reduced reticulocyte invasion by ∼50% in Brazilian and Thai clinical isolates in *ex vivo* invasion assays.[42]

The passive transfer experiments performed in this study support a major role for antibodies in protection. However, we cannot exclude the contribution of cellular immune responses. Previous studies in blood stage malaria models have shown that $CD4^+$ T cells can contribute to vaccine-induced protection, primarily by supporting the development and maintenance of humoral immunity, whereas the role of $CD8^+$ T cells appears to be more variable and often limited in the control of blood stage parasitemia.[43–45] Notably, in the first study describing E140 as a vaccine antigen, depletion of $CD4^+$ and/or $CD8^+$ T cells did not abolish protection, while passive transfer of immune serum delayed the onset of parasitemia, supporting a predominant role for antibody-mediated immunity.[9] Further studies will be required to define the exact contribution of cellular responses induced by E140 mRNA-LNP to vaccine-induced protection.

Building on our vaccination findings targeting the E140 antigen, the next step is to advance toward multi-antigen/multi-stage mRNA-LNP formulations that combine targets with complementary mechanisms, aiming for synergistic protection. This approach should broaden vaccine coverage and mitigate antigenic variability, increasing the likelihood of blocking parasites that evade single antigen-induced immunity.[46,47] Combining E140 with pre-erythrocytic and/or transmission-blocking antigens would also target various stages of the parasite's life cycle.[7,48,49]

Collectively, E140 mRNA-LNP vaccination yields a coherent immune profile with durable, balanced antibodies, robust B cell programming compatible with long-lived humoral immunity, *in vivo* protection, and *ex vivo* inhibition of *P. vivax* re-invasion, supporting E140 as a promising candidate for next-generation *P. vivax* vaccines using the nucleoside-modified mRNA-LNP vaccine technology.

MATERIALS AND ETHODS

E140 mRNA design and production

The sequences of the E140 protein from *P. berghei* and *P. vivax* were obtained from PlasmoDB: PBANKA_0209000 and PlasmoDB: PVP01_0210600, respectively.

Plasmids with codon-optimized sequences encoding PbE140, PvE140 and firefly luciferase (Luc) were synthesized (Genscript, Piscataway, NJ, USA). mRNAs were made as previously described.[50] Briefly, plasmids were linearized, and a T7-driven *in vitro* transcription reaction (Life Technologies, Carlsbad, CA, USA) was performed to generate mRNAs with 101 nucleotide long poly(A) tails. Capping of mRNAs was performed in concert with transcription through addition of a trinucleotide cap1 analog CleanCap, and m1Ψ-5′-triphosphate (TriLink, San Diego, CA, USA) was incorporated into the reaction instead of uridine-5′-triphosphate (UTP). Cellulose-based purification of mRNAs was performed as described[51] and the integrity of the purified mRNAs was evaluated on an agarose gel before storage at −20°C.

mRNA encapsulation to LNP

Cellulose-purified mRNAs were encapsulated in LNP using a self-assembly process where an aqueous solution of mRNAs at pH 4.0 is

rapidly mixed with a solution of lipids dissolved in ethanol. LNP used in this study consisted of a mixture of the ionizable cationic lipid (pKa in the range of 6.0–6.5, proprietary to Acuitas Therapeutics)/phosphatidylcholine/cholesterol/PEG-lipid as described in the patent application WO 2017/004143. Formulations were 76–79 nm in size as measured using Malvern Zetasizer (Malvern Panalytical, Worcestershire, UK) with encapsulation >96% as assayed using the Ribogreen assay (Life Technologies, Carlsbad, CA, USA).

Mouse immunizations

Female BALB/c mice, 8 weeks of age, were purchased from Charles River Laboratories (Wilmington, MA, USA) or the Faculty of Medicine, University of São Paulo (São Paulo, SP, Brazil). Mice were immunized i.m., with a 40 μL final volume with mRNA-LNPs encoding either PbE140, PvE140, or Luc in pohosphate buffered saline (PBS). Groups of mice were immunized with a single dose of 10 μg or two doses of 5 μg mRNA-LNP, 30 days apart. All animal experiments were approved by the Animal Care and Use Committee of the University of Pennsylvania and of the Institute of Biomedical Sciences of the University of São Paulo.

Recombinant protein production and purification

Recombinant *Plasmodium* proteins were expressed and purified as previously described in detail.[52] Briefly, the codon-optimized DNA fragments encoding the predicted extracellular regions of *P. vivax* E140 (aa 174–370, hereafter rPvE140) and PbE140 (aa 213–403, hereafter rPbE140) proteins were synthesized and cloned into pET-DUET-1 plasmid (cat. 71146–3; Merck Millipore, Burlington, MA, USA) with an N-terminal polyhistidine (His_6) tag. Chemically competent *Escherichia coli* (*E. coli*) SixPack cells were transformed and grown in LB broth supplemented with carbenicillin (100 μg/mL).[53] Cultures were induced at optical density (OD_{600}) = 0.5 with 1 mM isopropyl β-D-1-thiogalactopyranoside (IPTG) for 3 h at 37 °C (280 r.p.m.), harvested, washed in PBS, and lysed by sonication. Inclusion bodies were collected and washed sequentially with different detergent/urea-containing and detergent-free buffers, then solubilized by a modified single freeze-thaw method. After thawing, the clarified supernatant containing the recombinant protein was subjected to slow dilution-based refolding in a redox buffer system (4 °C, 24 h). Refolded and soluble recombinant PbE140 and PvE140 proteins were purified by immobilized metal ion affinity chromatography (IMAC) using Ni-Sepharose 6 Fast Flow resin (cat. 17531802; Cytiva, Marlborough, MA, USA), buffer-exchanged to 50 mM Tris pH 8.0 and 150 mM NaCl, concentrated to 1 mg/mL, flash frozen and stored at −80 °C until use. Protein integrity and purity were assessed by sodium dodecyl sulfate-polyacrylamide gel electrophoresis (SDS-PAGE) followed by Coomassie brilliant blue staining and immunoblotting, and protein sequences were validated by mass-spectrometric analysis.

ELISA

Twenty-five days after each immunization, blood was collected and sera were analyzed for the presence of antibodies recognizing the recombinant protein. Antibodies against PbE140 and PvE140 in mice sera were detected by ELISA as described previously.[54] Briefly, 96-well EIA/RIA Clear Flat Bottom Polystyrene High Bind Microplates (Corning Life Sciences, New York, NY, USA) were coated with recombinant PbE140 or PvE140 proteins in PBS (100 ng/well) and allowed to incubate overnight at 4°C. Plates were then washed three times with 0.05% Tween 20 (Sigma-Aldrich, St. Louis, Missouri, MO, USA) in PBS (PBS-T) and blocked with 2% BSA (Sigma-Aldrich, St. Louis, Missouri, MO, USA) in PBS (blocking buffer) for 1 h at room temperature (RT). After washing three times with PBS-T, serum samples were 3-fold serially diluted in blocking buffer and allowed to incubate at RT for 2 h. Plates were then washed three times with PBS-T, and HRP-conjugated anti-mouse IgG secondary antibody (Jackson ImmunoResearch Laboratories, West Grove, PA, USA) was added at a dilution of 1:10,000 in blocking buffer and incubated at RT for 1 h. Plates were then washed three times with PBS-T and developed using KPL 2-component TMB Microwell Peroxidase Substrate (Seracare, Milford, MA, USA) for 6 min before quenching with 2 N sulfuric acid (Sigma-Aldrich, St. Louis, Missouri, MO, USA). Detection of IgG subclass responses was performed as described above, except that HRP-conjugated anti-mouse IgG1, IgG2a, or IgG2b secondary antibodies (Southern Technologies Birmingham, AL, USA) were used. Absorbance was measured at 450 nm using a SpectraMax 190 microplate reader (Molecular Devices, San Jose, CA, USA). PbE140-or PvE140-specific IgG endpoint dilution titer was defined as the highest dilution of serum to give an OD greater than the sum of the background OD with 0.01 arbitrary units. All samples were run in technical duplicates.

Mapping of E140-specific B cell responses against *P. berghei* and *P. vivax*

Thirty days following immunization, spleens, and hind limb bone marrow were harvested from mice, processed, and enumerated for flow cytometric analysis. A total of 2×10^6 cells from either splenic or bone marrow compartments were stained to identify distinct B cell subpopulations, including: (1) total GC B cells (Live, $CD3^-$, $B220^+$, $GL7^+CD95^+$), (2) E140-specific GC B cells (Live, $CD3^-$, $B220^+$, $GL7^+CD95^+$, $E140^+$), (3) total plasma cells (Live, $CD3^-$, $B220^-CD138^+$), (4) E140-specific plasma cells (Live, CD3-, $B220^-CD138^+$, $E140^+$), (5) total plasmablasts (Live, $CD3^-$, $B220^+CD138^+$), and (6) E140-specific plasmablasts (Live, $CD3^-$, $B220^+CD138^+$, $E140^+$). The staining protocol was initiated by incubating cells with LIVE/DEAD Fixable Aqua Dead Cell Stain Kit in combination with 5 μg/mL of PbE140 or PbE140 recombinant proteins. Subsequently, cells were labeled with the following antibody panel: anti-CD3-APC-Cy7 (clone 145-2c11), anti-CD45R/B220-BV421 (clone RA3-6B2), anti-GL7-FITC (clone GL7), anti-CD95-PE (clone Jo2), anti-CD138-APC (clone 281–2), and anti-6×HisTag-Biotin (clone MA1-21315-BTN). The staining procedure was completed with streptavidin-BV421 conjugation. Flow cytometric acquisition was performed using a BD LSR Fortessa instrument, collecting 1×10^6 events per sample. Data analysis was conducted with FlowJo 10 software, focusing on the frequency of each cell population (frequency of parent). For comprehensive visualization of the multiparameter flow cytometry data, TriMap dimensionality reduction

analysis was employed.[55] The method operates by incorporating triplet relationships of the form (i, j, k), where point i is closer to point j than point k, allowing for superior preservation of the overall data structure including cluster placement and hierarchical relationships.

Mouse *Plasmodium* challenge and parasitemia analyses

Thirty days after administration of the last vaccine dose, mice were challenged intravenously (i.v.) with 5×10^3 erythrocytes parasitized with *Pb*NK65, obtained from previously infected donor mice. Parasitemia was monitored every other day after challenge. Blood smears were prepared on glass slides with a drop of blood obtained from mouse tail veins, fixed with methanol and stained for 15 min using 10% Giemsa. The glass slides were observed under a light microscope, and the percentages of parasitized red blood cells were determined by microscopic examination of stained blood smears. Mice were euthanized when signs (one or more) of severe disease/illness were observed, characterized by ruffled fur, shivering, weight loss, irregular breathing, and difficulty to walk.[56]

Passive serum transfer

The passive serum transfer assay was conducted as described,[57] with specific modifications implemented. Briefly, mice were immunized i.m. twice with a 30-day interval with 5 μg of PbE140 mRNA-LNP or Luc mRNA-LNP. Thirty days after the second immunization, mice were euthanized and blood was collected. The blood was allowed to coagulate at RT for 1 h before being placed at 4°C for 30 min. Serum was isolated by centrifuging the blood samples at 12,000 × *g* for 10 min at 4 °C, pooled and stored at −20 °C until used. Naive mice were i.v. injected with 200 μL of sera 2 h prior to the challenge, and a second serum transfer was performed 5 days post challenge. To confirm successful antibody transfer, blood samples were collected approximately 8 h after serum administration to naive animals, and antigen-specific IgG titers were determined by ELISA.

Antibody-mediated re-invasion inhibition assay

Human samples

Peripheral blood (30 mL) from untreated *P. vivax* malaria patients was collected by venipuncture into ACD (citrate-dextrose) tubes following approval by the Research Ethics Committee of the Federal University of Rondonia (CAAE: 56853922.2.0000.5300) and written informed consent. Human serum from healthy donors with AB blood type was obtained for media supplementation and controls. Baseline parasitemia and stage of maturation were determined on thick blood films, counting the parasite number per 200 white blood cells (WBCs) and calculating parasites per μL using the formula: (number of parasites counted × 8,000)/number of WBCs counted.

Reticulocyte enrichment

Venous whole blood from healthy donors collected in heparin tubes (100 mL) was centrifuged at 400 × *g* for 4 min at 20°C–24°C, the plasma was removed, and the blood was washed once with Iscove's modified Dulbecco's medium (IMDM) culture medium. Subsequently, the hematocrit was adjusted to 50%, and the blood was passed through a CF11 cellulose column.[58] The leukocyte-depleted effluent was washed once with IMDM and subjected to reticulocyte enrichment using 65% Percoll. For the gradient, 5 mL 65% Percoll was mixed 1:1 with 5 mL blood and centrifuged with 300 s acceleration/300 s deceleration for 15 min at 1,200 × *g* at 20°C–24°C, avoiding abrupt braking. The interphase (reticulocyte-enriched ring) was collected, washed once with IMDM, and the hematocrit adjusted to 50% in complete IMDM. Purified reticulocytes were stained with cresyl blue dye, and the percentage of reticulocytes was determined.

Parasite maturation and schizont enrichment

2 mL of *P. vivax*-infected RBC (Pv-iRBC) pellet was brought to 14 mL with complete IMDM (20% AB serum) in T-75 flasks. Flasks were flushed for 10 s with 90% N_2/5% CO_2/5% O_2, sealed, and incubated at 37 °C for 16–24 h, adjusted to the predominant initial stage of maturation.[59] Progression to schizonts was confirmed on thick blood films stained with giemsa. When cultures reached at least 50% maturation, schizonts were enriched using 45% Percoll by centrifugation (1,200 × *g*, 15 min); the enriched fraction was collected, washed twice with IMDM, and the cell concentration was adjusted to 50 μL in complete IMDM.

Re-invasion inhibition assay

Assays were performed in 96-well U-bottom plates targeting a 2% hematocrit and a final volume of 200 μL/well. For each well, a 1:1 mixture of schizont-enriched Pv-iRBCs and reticulocytes was added (5 μL iRBC +5 μL reticulocytes) and brought to final volume with complete IMDM. Sera from mice immunized with two doses of 5 μg PvE140 mRNA-LNP were tested at 1:10 dilution. Controls included AB human serum (matrix control) and a negative control serum from animals immunized with Luc mRNA-LNP control vaccine. Plates were flushed with 90% N_2/5% CO_2/5% O_2 and incubated overnight (18–24 h) at 37 °C in hypoxic chambers to allow egress and re-invasion.[60]

At the end of incubation, wells were gently mixed and thin blood smears were prepared, methanol-fixed, and stained with 10% Giemsa. For each condition, ≥5,000 RBCs (or ≥30 high-power fields at 100× oil) were counted to determine ring-stage parasitemia as a readout of re-invasion. Parasitemia (P) was calculated as (ring-infected RBCs/total RBCs) × 100. Percent inhibition was calculated as % inhibition = 100 × [1 − (P_treatment/P_control)].

Ethics statement

Mouse studies complied with the NIH guide for the care and use of laboratory animals and were conducted in accredited facilities. Protocols were approved by the Institutional Animal Care and Use Committee (IACUC) at the University of Pennsylvania (protocol number 807165) and by the Institutional Animal Care and Use Committee (CEUA) at the Institute of Biomedical Sciences of the University of São Paulo (protocol number 4395240122).

Statistics and analysis

One-way ANOVA followed by Tukey's test, or log rank (Mantel-Cox) test, were used to calculate statistical significance (*p* values).

Prism 10 software (GraphPad Software Inc., LA Jolla, CA) was used for all tests and differences were considered significant when $p \leq 0.05$.

DATA AND CODE AVAILABILITY

All data are available within the article and its supplemental information file or from the corresponding authors upon request.

ACKNOWLEDGMENTS

This study was supported by São Paulo Research Foundation (FAPESP) with a grant awarded to D.Y.B. (2021/06769-0), and fellowships to R.F.M. (2021/04455-9 and 2022/15895-2) and G.A.d.S.-S. (2022/00204-4).

The Pardi laboratory was supported by the National Institute of Allergy and Infectious Diseases (NIAID; R01AI153064, P01AI158571 and U19AI181968). Z.L. was supported by the National Laboratory for Biotechnology (2022-2.1.1-NL-2022-00008), the Hungarian Academy of Sciences (Lendület program grant LP2017-7/2017) and partially by the 2021-1.1.4-GYORSÍTÓSÁV-2022-00008 project of NRDI Office, Hungary. The authors are grateful for the Single Cell Omics Advanced Core Facility staff of the HCEMM (supported by the EU Horizon 2020 grant (no. 739593) and NRDI Office, Hungary (no. 2022-2.1.1-NL-2022-00005) and HUN-REN BRC for the mass spectrometric validation of the recombinant proteins.

AUTHOR CONTRIBUTIONS

D.Y.B., N.P., and R.F.M. conceived the study; D.Y.B., N.P., R.F.M., G.A.d.S.-S., V.A.d.S., A.S., M.V., E.A., Z.L., and A.C.C.A. designed and performed experiments; D.Y.B., N.P., R.F.M., G.A.d.S.-S., M.V., A.S., S.B.B., C.B.G., Z.L., and A.C.C.A. reviewed and interpreted data; H.M. and R.H.J.J. contributed to vaccine production; D.Y.B., N.P., and R.F.M. drafted the manuscript, all other authors edited the paper. All authors had access to data and gave final approval before submission.

DECLARATION OF INTERESTS

N.P. is named on patents describing the use of nucleoside-modified mRNA in LNPs as a vaccine platform. He has disclosed those interests fully to the University of Pennsylvania, and he has in place an approved plan for managing any potential conflicts arising from licensing of those patents. N.P. served on the mRNA strategic advisory board of Sanofi Pasteur in 2022, Pfizer in 2023–2024 and AldexChem in 2023–2025. N.P. is a member of the Scientific Advisory Board of BioNet, and has consulted for Vaccine Company Inc., Pasture Bio, and Piezo Therapeutics. Z.L. held consulting positions at ATGandCo Biotechnology Ltd. when the study was conceived, but the company did not contribute to the funding, design, or execution of the research, nor to the preparation of the manuscript.

SUPPLEMENTAL INFORMATION

Supplemental information can be found online at https://doi.org/10.1016/j.omtn.2026.103083.

REFERENCES

1. World Health Organization (2024). World Malaria Report 2024 (World Health Organization).
2. González-Sanz, M., Berzosa, P., and Norman, F.F. (2023). Updates on Malaria Epidemiology and Prevention Strategies. Curr. Infect. Dis. Rep. 1–9. https://doi.org/10.1007/s11908-023-00805-9.
3. Haldar, K., Bhattacharjee, S., and Safeukui, I. (2018). Drug resistance in Plasmodium. Nat. Rev. Microbiol. *16*, 156–170. https://doi.org/10.1038/nrmicro.2017.161.
4. Suh, P.F., Elanga-Ndille, E., Tchouakui, M., Sandeu, M.M., Tagne, D., Wondji, C., and Ndo, C. (2023). Impact of insecticide resistance on malaria vector competence: a literature review. Malar. J. *22*, 19. https://doi.org/10.1186/s12936-023-04444-2.
5. da Veiga, G.T.S., Moriggi, M.R., Vettorazzi, J.F., Müller-Santos, M., and Albrecht, L. (2022). *Plasmodium vivax* vaccine: What is the best way to go? Front. Immunol. *13*, 910236. https://doi.org/10.3389/fimmu.2022.910236.
6. Oduoye, M.O., Haider, M.U., Marsool, M.D.M., Kareem, M.O., Adedayo, A.E., Abdulkarim, A.S., Adegoke, A.A., Kaushik, I., Irfan, H., Yusuf, H.A., et al. (2024). Unlocking the potential of novel RTS, S/AS01, and R21/Matrix-M malaria vaccines in African nations. Health Sci. Rep. *7*, e1797. https://doi.org/10.1002/hsr2.1797.
7. De, S.L., Ntumngia, F.B., Nicholas, J., and Adams, J.H. (2021). Progress towards the development of a *P. vivax* vaccine. Expert Rev. Vaccines *20*, 97–112. https://doi.org/10.1080/14760584.2021.1880898.
8. Tachibana, M., Takashima, E., Morita, M., Sattabongkot, J., Ishino, T., Culleton, R., Torii, M., and Tsuboi, T. (2022). *Plasmodium vivax* transmission-blocking vaccines: Progress, challenges and innovation. Parasitol. Int. *87*, 102525. https://doi.org/10.1016/j.parint.2021.102525.
9. Smith, E.C., Limbach, K.J., Rangel, N., Oda, K., Bolton, J.S., Du, M., Gowda, K., Wang, J., Moch, J.K., Sonawane, S., et al. (2020). Novel malaria antigen *Plasmodium yoelii* E140 induces antibody-mediated sterile protection in mice against malaria challenge. PLoS One *15*, e0232234. https://doi.org/10.1371/journal.pone.0232234.
10. Howick, V.M., Russell, A.J.C., Andrews, T., Heaton, H., Reid, A.J., Natarajan, K., Butungi, H., Metcalf, T., Verzier, L.H., Rayner, J.C., et al. (2019). The Malaria Cell Atlas: Single parasite transcriptomes across the complete Plasmodium life cycle. Science *365*, eaaw2619. https://doi.org/10.1126/science.aaw2619.
11. Pardi, N., and Krammer, F. (2024). mRNA vaccines for infectious diseases - advances, challenges and opportunities. Nat. Rev. Drug Discov. *23*, 838–861. https://doi.org/10.1038/s41573-024-01042-y.
12. Cowman, A.F., Healer, J., Marapana, D., and Marsh, K. (2016). Malaria: Biology and Disease. Cell *167*, 610–624. https://doi.org/10.1016/j.cell.2016.07.055.
13. Adams, J.H., and Mueller, I. (2017). The Biology of *Plasmodium vivax*. Cold Spring Harb. Perspect. Med. *7*, a025585. https://doi.org/10.1101/cshperspect.a025585.
14. Limsalakpetch, A., Kum-Arb, U., Yongvanitchit, K., Im-Erbsin, R., Ubalee, R., Waters, N., Vesely, B.A., Muramatsu, H., Weissman, D., Tam, Y.K., et al. (2025). mRNA-LNP vaccine encoding the *Plasmodium vivax* circumsporozoite protein is highly immunogenic and confers protection in mice. Mol. Ther. Nucleic Acids *36*, 102645. https://doi.org/10.1016/j.omtn.2025.102645.
15. Kunkeaw, N., Nguitragool, W., Takashima, E., Kangwanrangsan, N., Muramatsu, H., Tachibana, M., Ishino, T., Lin, P.J.C., Tam, Y.K., Pichyangkul, S., et al. (2023). A Pvs25 mRNA vaccine induces complete and durable transmission-blocking immunity to *Plasmodium vivax*. NPJ Vaccines *8*, 187. https://doi.org/10.1038/s41541-023-00786-9.
16. Lasonder, E., Janse, C.J., van Gemert, G.J., Mair, G.R., Vermunt, A.M.W., Douradinha, B.G., van Noort, V., Huynen, M.A., Luty, A.J.F., Kroeze, H., et al. (2008). Proteomic profiling of Plasmodium sporozoite maturation identifies new proteins essential for parasite development and infectivity. PLoS Pathog. *4*, e1000195. https://doi.org/10.1371/journal.ppat.1000195.
17. Ebrahimpoor, S., Pakzad, S.R., and Ajdary, S. (2013). IgG1 and IgG2a profile of serum antibodies to Leishmania major amastigote in BALB/c and C57BL/6Mice. Iran. J. Allergy Asthma Immunol. *12*, 361–367.
18. Petrović, R., Bufan, B., Arsenović-Ranin, N., Živković, I., Minić, R., Radojević, K., and Leposavić, G. (2018). Mouse strain and sex as determinants of immune response to trivalent influenza vaccine. Life Sci. *207*, 117–126. https://doi.org/10.1016/j.lfs.2018.05.056.
19. Amemiya, K., Bush, G.V., DeShazer, D., and Waag, D.M. (2002). Nonviable Burkholderia mallei induces a mixed Th1- and Th2-like cytokine response in BALB/c mice. Infect. Immun. *70*, 2319–2325. https://doi.org/10.1128/IAI.70.5.2319-2325.2002.
20. Fornefett, J., Krause, J., Klose, K., Fingas, F., Hassert, R., Benga, L., Grunwald, T., Müller, U., Schrödl, W., and Baums, C.G. (2018). Comparative analysis of humoral immune responses and pathologies of BALB/c and C57BL/6 wildtype mice experimentally infected with a highly virulent Rodentibacter pneumotropicus (Pasteurella pneumotropica) strain. BMC Microbiol. *18*, 45. https://doi.org/10.1186/s12866-018-1186-8.
21. Waki, S., Uehara, S., Kanbe, K., Nariuch, H., and Suzuki, M. (1995). Interferon-gamma and the induction of protective IgG2a antibodies in non-lethal *Plasmodium berghei* infections of mice. Parasite Immunol. *17*, 503–508. https://doi.org/10.1111/j.1365-3024.1995.tb00880.x.

22. White, W.I., Evans, C.B., and Taylor, D.W. (1991). Antimalarial antibodies of the immunoglobulin G2a isotype modulate parasitemias in mice infected with *Plasmodium yoelii*. Infect. Immun. *59*, 3547–3554. https://doi.org/10.1128/iai.59.10.3547-3554.1991.

23. Rathay, V., Fürle, K., Kiehl, V., Ulmer, A., Lanzer, M., and Thomson-Luque, R. (2024). IgG Subclass Switch in Volunteers Repeatedly Immunized with the Full-Length *Plasmodium falciparum* Merozoite Surface Protein 1 (MSP1). Vaccines (Basel) *12*, 208. https://doi.org/10.3390/vaccines12020208.

24. Seaton, K.E., Spreng, R.L., Abraha, M., Reichartz, M., Rojas, M., Feely, F., 2nd, Jongert, E., Coccia, M., Ulloa-Montoya, F., Wille-Reece, U., et al. (2021). Subclass and avidity of circumsporozoite protein specific antibodies associate with protection status against malaria infection. NPJ Vaccines *6*, 110. https://doi.org/10.1038/s41541-021-00372-x.

25. Ubillos, I., Ayestaran, A., Nhabomba, A.J., Dosoo, D., Vidal, M., Jiménez, A., Jairoce, C., Sanz, H., Aguilar, R., Williams, N.A., et al. (2018). Baseline exposure, antibody subclass, and hepatitis B response differentially affect malaria protective immunity following RTS,S/AS01E vaccination in African children. BMC Med. *16*, 197. https://doi.org/10.1186/s12916-018-1186-4.

26. Ndungu, F.M., Bull, P.C., Ross, A., Lowe, B.S., Kabiru, E., and Marsh, K. (2002). Naturally acquired immunoglobulin (Ig)G subclass antibodies to crude asexual *Plasmodium falciparum* lysates: evidence for association with protection for IgG1 and disease for IgG2. Parasite Immunol. *24*, 77–82. https://doi.org/10.1046/j.0141-9838.2001.00440.x.

27. Roussilhon, C., Oeuvray, C., Müller-Graf, C., Tall, A., Rogier, C., Trape, J.F., Theisen, M., Balde, A., Pérignon, J.L., and Druilhe, P. (2007). Long-term clinical protection from falciparum malaria is strongly associated with IgG3 antibodies to merozoite surface protein 3. PLoS Med. *4*, e320. https://doi.org/10.1371/journal.pmed.0040320.

28. Kana, I.H., Garcia-Senosiain, A., Singh, S.K., Tiendrebeogo, R.W., Chourasia, B.K., Malhotra, P., Sharma, S.K., Das, M.K., Singh, S., Adu, B., and Theisen, M. (2018). Cytophilic Antibodies Against Key *Plasmodium falciparum* Blood Stage Antigens Contribute to Protection Against Clinical Malaria in a High Transmission Region of Eastern India. J. Infect. Dis. *218*, 956–965. https://doi.org/10.1093/infdis/jiy258.

29. Feehan, J., Plebanski, M., and Apostolopoulos, V. (2025). Recent perspectives in clinical development of malaria vaccines. Nat. Commun. *16*, 3565. https://doi.org/10.1038/s41467-025-58963-4.

30. Kumar, K.A., Sano, G.i., Boscardin, S., Nussenzweig, R.S., Nussenzweig, M.C., Zavala, F., and Nussenzweig, V. (2006). The circumsporozoite protein is an immunodominant protective antigen in irradiated sporozoites. Nature *444*, 937–940. https://doi.org/10.1038/nature05361.

31. Boyle, M.J., Chan, J.A., Handayuni, I., Reiling, L., Feng, G., Hilton, A., Kurtovic, L., Oyong, D., Piera, K.A., Barber, B.E., et al. (2019). IgM in human immunity to *Plasmodium falciparum* malaria. Sci. Adv. *5*, eaax4489. https://doi.org/10.1126/sciadv.aax4489.

32. Rosenkranz, M., Fürle, K., Hibbert, J., Ulmer, A., Ali, A., Giese, T., Blank, A., Haefeli, W.E., Böhnlein, E., Lanzer, M., and Thomson-Luque, R. (2023). Multifunctional IgG/IgM antibodies and cellular cytotoxicity are elicited by the full-length MSP1 SumayaVac-1 malaria vaccine. NPJ Vaccines *8*, 112. https://doi.org/10.1038/s41541-023-00701-2.

33. Turner, J.S., O'Halloran, J.A., Kalaidina, E., Kim, W., Schmitz, A.J., Zhou, J.Q., Lei, T., Thapa, M., Chen, R.E., Case, J.B., et al. (2021). SARS-CoV-2 mRNA vaccines induce persistent human germinal centre responses. Nature *596*, 109–113. https://doi.org/10.1038/s41586-021-03738-2.

34. Kim, W., Zhou, J.Q., Horvath, S.C., Schmitz, A.J., Sturtz, A.J., Lei, T., Liu, Z., Kalaidina, E., Thapa, M., Alsoussi, W.B., et al. (2022). Germinal centre-driven maturation of B cell response to mRNA vaccination. Nature *604*, 141–145. https://doi.org/10.1038/s41586-022-04527-1.

35. Robinson, M.J., Dowling, M.R., Pitt, C., O'Donnell, K., Webster, R.H., Hill, D.L., Ding, Z., Dvorscek, A.R., Brodie, E.J., Hodgkin, P.D., et al. (2022). Long-lived plasma cells accumulate in the bone marrow at a constant rate from early in an immune response. Sci. Immunol. *7*, eabm8389. https://doi.org/10.1126/sciimmunol.abm8389.

36. Plotkin, S.A. (2010). Correlates of protection induced by vaccination. Clin. Vaccine Immunol. *17*, 1055–1065. https://doi.org/10.1128/CVI.00131-10.

37. Nguyen, D.C., Hentenaar, I.T., Morrison-Porter, A., Solano, D., Haddad, N.S., Castrillon, C., Runnstrom, M.C., Lamothe, P.A., Andrews, J., Roberts, D., et al. (2025). SARS-CoV-2-specific plasma cells are not durably established in the bone marrow long-lived compartment after mRNA vaccination. Nat. Med. *31*, 235–244. https://doi.org/10.1038/s41591-024-03278-y.

38. Guo, C., Chai, X., Baerlike, M., Liu, Y., Wang, Y., Shao, F., Huang, Q., Zhang, W., Cen, S., Dong, Y., et al. (2024). Comparison of antigen-specific B cell responses reveals disparity in immunogenicity and memory B cell formation across COVID-19 vaccine platforms. hLife *2*, 625–640. https://doi.org/10.1016/j.hlife.2024.09.002.

39. Pardi, N., Hogan, M.J., Naradikian, M.S., Parkhouse, K., Cain, D.W., Jones, L., Moody, M.A., Verkerke, H.P., Myles, A., Willis, E., et al. (2018). Nucleoside-modified mRNA vaccines induce potent T follicular helper and germinal center B cell responses. J. Exp. Med. *215*, 1571–1588. https://doi.org/10.1084/jem.20171450.

40. Grimberg, B.T., Udomsangpetch, R., Xainli, J., McHenry, A., Panichakul, T., Sattabongkot, J., Cui, L., Bockarie, M., Chitnis, C., Adams, J., et al. (2007). *Plasmodium vivax* invasion of human erythrocytes inhibited by antibodies directed against the Duffy binding protein. PLoS Med. *4*, e337. https://doi.org/10.1371/journal.pmed.0040337.

41. Carias, L.L., Dechavanne, S., Nicolete, V.C., Sreng, S., Suon, S., Amaratunga, C., Fairhurst, R.M., Dechavanne, C., Barnes, S., Witkowski, B., et al. (2019). Identification and Characterization of Functional Human Monoclonal Antibodies to *Plasmodium vivax* Duffy-Binding Protein. J. Immunol. *202*, 2648–2660. https://doi.org/10.4049/jimmunol.1801631.

42. Chan, L.J., Gandhirajan, A., Carias, L.L., Dietrich, M.H., Vadas, O., Visentin, R., França, C.T., Menant, S., Soldati-Favre, D., Mueller, I., et al. (2021). Naturally acquired blocking human monoclonal antibodies to *Plasmodium vivax* reticulocyte binding protein 2b. Nat. Commun. *12*, 1538. https://doi.org/10.1038/s41467-021-21811-2.

43. Raja, A.I., Cai, Y., Reiman, J.M., Groves, P., Chakravarty, S., McPhun, V., Doolan, D.L., Cockburn, I., Hoffman, S.L., Stanisic, D.I., and Good, M.F. (2016). Chemically Attenuated Blood-Stage *Plasmodium yoelii* Parasites Induce Long-Lived and Strain-Transcending Protection. Infect. Immun. *84*, 2274–2288. https://doi.org/10.1128/IAI.00157-16.

44. Stanisic, D.I., Ho, M.F., Nevagi, R., Cooper, E., Walton, M., Islam, M.T., Hussein, W.M., Skwarczynski, M., Toth, I., and Good, M.F. (2021). Development and Evaluation of a Cryopreserved Whole-Parasite Vaccine in a Rodent Model of Blood-Stage Malaria. mBio *12*, e0265721. https://doi.org/10.1128/mBio.02657-21.

45. Demarta-Gatsi, C., Peronet, R., Smith, L., Thiberge, S., Ménard, R., and Mécheri, S. (2017). Immunological memory to blood-stage malaria infection is controlled by the histamine releasing factor (HRF) of the parasite. Sci. Rep. *7*, 9129. https://doi.org/10.1038/s41598-017-09684-2.

46. Bustamante, L.Y., Powell, G.T., Lin, Y.C., Macklin, M.D., Cross, N., Kemp, A., Cawkill, P., Sanderson, T., Crosnier, C., Muller-Sienerth, N., et al. (2017). Synergistic malaria vaccine combinations identified by systematic antigen screening. Proc. Natl. Acad. Sci. USA *114*, 12045–12050. https://doi.org/10.1073/pnas.1702944114.

47. Atapour, A., Vosough, P., Jafari, S., and Sarab, G.A. (2022). A multi-epitope vaccine designed against blood-stage of malaria: an immunoinformatic and structural approach. Sci. Rep. *12*, 11683. https://doi.org/10.1038/s41598-022-15956-3.

48. Theisen, M., Roeffen, W., Singh, S.K., Andersen, G., Amoah, L., van de Vegte-Bolmer, M., Arens, T., Tiendrebeogo, R.W., Jones, S., Bousema, T., et al. (2014). A multi-stage malaria vaccine candidate targeting both transmission and asexual parasite life-cycle stages. Vaccine *32*, 2623–2630. https://doi.org/10.1016/j.vaccine.2014.03.020.

49. Chick, J.A., Abongdia, N.N., Shey, R.A., and Apinjoh, T.O. (2025). Computational design, expression, and characterization of a *Plasmodium falciparum* multi-epitope, multi-stage vaccine candidate (PfCTMAG). Heliyon *11*, e42014. https://doi.org/10.1016/j.heliyon.2025.e42014.

50. Vadovics, M., Muramatsu, H., Sárközy, A., and Pardi, N. (2024). Production and Evaluation of Nucleoside-Modified mRNA Vaccines for Infectious Diseases. Methods Mol. Biol. *2786*, 167–181. https://doi.org/10.1007/978-1-0716-3770-8_7.

51. Baiersdörfer, M., Boros, G., Muramatsu, H., Mahiny, A., Vlatkovic, I., Sahin, U., and Karikó, K. (2019). A Facile Method for the Removal of dsRNA Contaminant from

In Vitro-Transcribed mRNA. Mol. Ther. Nucleic Acids *15*, 26–35. https://doi.org/10.1016/j.omtn.2019.02.018.

52. Marques, R.F., Ábrahám, E., Muramatsu, H., Bargieri, D.Y., Pardi, N., and Lipinszki, Z. (2025). Expression and purification of E140 protein antigen fragments of *Plasmodium vivax* and *Plasmodium berghei* for serological assays. FEBS Open Bio *15*, 690–698. https://doi.org/10.1002/2211-5463.13939.

53. Lipinszki, Z., Vernyik, V., Farago, N., Sari, T., Puskas, L.G., Blattner, F.R., Posfai, G., and Gyorfy, Z. (2018). Enhancing the Translational Capacity of E. coli by Resolving the Codon Bias. ACS Synth. Biol. *7*, 2656–2664. https://doi.org/10.1021/acssynbio.8b00332.

54. Pine, M., Arora, G., Hart, T.M., Bettini, E., Gaudette, B.T., Muramatsu, H., Tombácz, I., Kambayashi, T., Tam, Y.K., Brisson, D., et al. (2023). Development of an mRNA-lipid nanoparticle vaccine against Lyme disease. Mol. Ther. *31*, 2702–2714. https://doi.org/10.1016/j.ymthe.2023.07.022.

55. Amid, E., and Warmuth, M.K. (2022). TriMap: Large-scale Dimensionality Reduction Using Triplets. Preprint at arXiv. https://doi.org/10.48550/arXiv.1910.00204.

56. Dobrescu, I., de Camargo, T.M., Gimenez, A.M., Murillo, O., Amorim, K.N.d.S., Marinho, C.R.F., Soares, I.S., Boscardin, S.B., and Bargieri, D.Y. (2020). Protective Immunity in Mice Immunized With *P. vivax* MSP1(19)-Based Formulations and Challenged With P. berghei Expressing PvMSP1(19). Front. Immunol. *11*, 28. https://doi.org/10.3389/fimmu.2020.00028.

57. Pardi, N., Carreño, J.M., O'Dell, G., Tan, J., Bajusz, C., Muramatsu, H., Rijnink, W., Strohmeier, S., Loganathan, M., Bielak, D., et al. (2022). Development of a pentavalent broadly protective nucleoside-modified mRNA vaccine against influenza B viruses. Nat. Commun. *13*, 4677. https://doi.org/10.1038/s41467-022-32149-8.

58. Sriprawat, K., Kaewpongsri, S., Suwanarusk, R., Leimanis, M.L., Lek-Uthai, U., Phyo, A.P., Snounou, G., Russell, B., Renia, L., and Nosten, F. (2009). Effective and cheap removal of leukocytes and platelets from *Plasmodium vivax* infected blood. Malar. J. *8*, 115. https://doi.org/10.1186/1475-2875-8-115.

59. Russell, B.M., Udomsangpetch, R., Rieckmann, K.H., Kotecka, B.M., Coleman, R.E., and Sattabongkot, J. (2003). Simple in vitro assay for determining the sensitivity of *Plasmodium vivax* isolates from fresh human blood to antimalarials in areas where *P. vivax* is endemic. Antimicrob. Agents Chemother. *47*, 170–173. https://doi.org/10.1128/AAC.47.1.170-173.2003.

60. Russell, B., Suwanarusk, R., Borlon, C., Costa, F.T.M., Chu, C.S., Rijken, M.J., Sriprawat, K., Warter, L., Koh, E.G.L., Malleret, B., et al. (2011). A reliable ex vivo invasion assay of human reticulocytes by *Plasmodium vivax*. Blood *118*, e74–e81. https://doi.org/10.1182/blood-2011-04-348748.